HHS Public Access

Author manuscript

J Am Chem Soc. Author manuscript; available in PMC 2020 November 06.

Published in final edited form as:

J Am Chem Soc. 2019 November 06; 141(44): 17909–17917. doi:10.1021/jacs.9b09671.

Self-Healing Heterometallic Supramolecular Polymers Constructed by Hierarchical Assembly of Triply Orthogonal Interactions with Tunable Photophysical Properties

Qian Zhang[†,‡,#], **Danting Tang**[†,#], **Jinjin Zhang**[†], **Ruidong Ni**[§], **Luonan Xu**[†], **Tian He**[†], **Xiongjie Lin**[†], **Xiaopeng Li**[§], **Huayu Qiu**[†], **Shouchun Yin**[*,†], **Peter J. Stang**[*,‡]

[†]College of Materials, Chemistry and Chemical Engineering, Hangzhou Normal University, Hangzhou 310036, P. R. China.

[‡]Department of Chemistry, University of Utah, 315 South 1400 East, Room 2020, Salt Lake City, Utah 84112, United States.

[§]Department of Chemistry, University of South Florida, 4202 East Fowler Avenue, Tampa, Florida 33620, United States.

Abstract

Here we present a method for the building of new bicyclic heterometallic cross-linked supramolecular polymers by hierarchical unification of three types of orthogonal noncovalent interactions, including platinum(II)-pyridine coordination-driven self-assembly, zinc-terpyridine complex and host–guest interactions. The platinum-pyridine coordination provides the primary driving force to form discrete rhomboidal metallacycles. The assembly doesn't interfere with the zinc-terpyridine complexes, which link the discrete metallacycles into linear supramolecular polymers, and the conjugation length is extended upon the formation of the zinc-terpyridine complexes, which redshifts the absorption and emission spectra. Finally, host-guest interactions via bis-ammonium salt binding to the benzo-21-crown-7 (B21C7) groups on the platinum acceptors afford the cross-linked supramolecular polymers. By continuous increase of the concentration of the supramolecular polymer to a relatively high level, supramolecular polymer gel is obtained, which exhibits self-healing properties and reversible gel–sol transitions stimulated by various external stimuli, including temperature, K^+ and cyclen. Moreover, the photophysical properties of the supramolecular polymers could be effectively tuned by varying the substituents of the precursor ligands.

Graphical Abstract

[*]**Corresponding Authors**: yinsc@hznu.edu.cn, stang@chem.utah.edu.

[#]Q.Z. and D.T. contributed equally to this work.

There are no conflicts to declare.

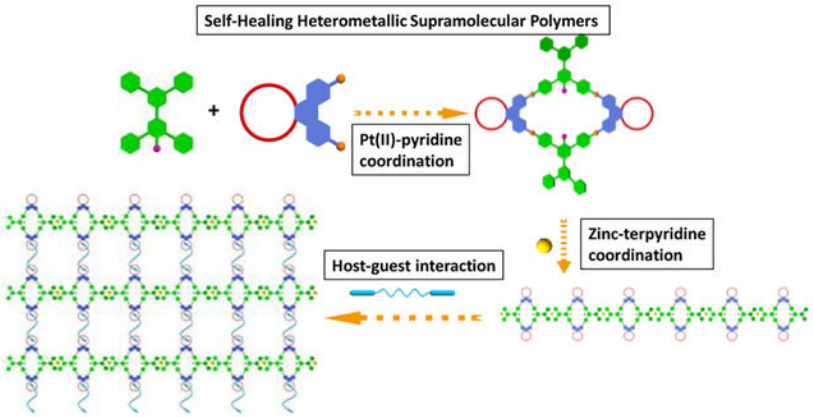

INTRODUCTION

Supramolecular polymers,[1] i.e. polymeric arrays of monomer units that are assembled by reversible and highly directional noncovalent bonds, have gained remarkable attention due to the combination of the conventional polymeric properties and the fascinating features like stimuli-responsive and self-healing capabilities.[2–9] The dynamic properties of these materials deriving from the reversible noncovalent bonds make supramolecular polymers attractive for various applications, such as drug delivery, biosensors, tissue engineering, optical devices, actuators and coatings and textiles.[10–15]

Among the miscellaneous noncovalent interactions, such as metal-ligand coordination, host-guest interactions, H-bonding, π-π stacking, van der Waals forces, hydrophobic forces, etc, metal-ligand coordination is of particular interest due to its high directionality and strong strength approaching that of covalent bonds.[16–18] Metal-ligand coordination has been demonstrated to be an efficient strategy for preparing supramolecular polymers since it allows the construction of well-defined supramolecular architectures and endows the resulting polymers with higher stability in comparison with other noncovalent interactions.[19–21] Meanwhile, coordination-driven polymers could combine the properties of organic polymers with the photophysical, magnetic, electronic, and catalytic potential of metals. The chemistry of metal-terpyridine complexes is a particularly powerful tool for the building of supramolecular architectures and polymers, since terpyridine moieties are capable of forming strong, directed and reversible complexes with a variety of metal ions due to dπ-pπ* back-bonding of the metal to pyridine rings and the chelate effect.[22–28] For example, Schubert and coworkers reported a linear water-soluble metallo-supramolecular polymer based on iron(II)/terpyridine complexes, which showed high thermal stability and reversible properties.[22]

Supramolecular polygons and polyhedrons with well-defined sizes, shapes and geometries could be readily constructed via the metal-ligand coordination-driven self-assembly.[29–42] Using a selective and reasonable choice of precursors, Stang,[29] Fujita,[30] Raymond,[33] Nitschke,[28] and others have designed and synthesized a library of elegant two-dimensional metallacycles and three-dimensional metallacages, which are increasingly of interest in various applications such as encapsulation, catalysis, chemosensing, and light harvesting.

Because of the well-defined structures of metallacycles, multiple functional moieties can be easily covalently appended either on the periphery or at the vertices of predesigned metallacyclic skeletons, which afford the chance to introduce other types of noncovalent interactions for orthogonal hierarchical self-assembly.[43–46] Via orthogonal combination of metal-ligand coordination-driven self-assembly with other different noncovalent interactions, multifunctional metallacycle- or metallacage-cored supramolecular polymers could be readily accessed.[16,45,47] For example, Stang and coworkers reported several functional supramolecular polymers with fascinating properties by the unification of platinum(II)-ligand coordination-driven self-assembly with hydrogen bonding or crown ether-based host–guest interactions.[43,48–50] However, it is still very challenging to prepare the well-controlled hierarchical self-assembly of organometallic materials with higher-order structures, especially the stimuli-responsive smart soft materials. Superstructures assembled via three or more types of orthogonal noncovalent interactions that do not interfere with one another, are rarely reported.[51] Up to now, usually only one type of metal-ligand binding motif was incorporated in those structures. It is intriguing to functionalize the architectures with secondary metal sites, which could furnish the materials with more novel functionalities, such as electrochemical, photophysical or magnetic properties.[52]

Herein, in addition to platinum(II)←pyridine coordination motif, we introduced a second coordination motif, the terpyridine-zinc(II) complex to the backbone of the supramolecular polymers. To this end, a heterometallic cross-linked supramolecular polymer was constructed by the hierarchical unification of three types of noncovalent interactions, platinum(II)-ligand coordination-driven self-assembly, zinc(II)-terpyridine complex and host–guest interactions. As shown in Scheme 1, ditopic ligands with one end terminating with a terpyridyl moiety and the other terminating with a 120° dipyridyl fragment, bearing different substituents were synthesized, wherein platinum(II) could bind to the 120° dipyridyl moiety to form rhomboidal metallacycles, and then the terminal terpyridines can coordinate with Zn(II) into linear supramolecular polymers. To the best of our knowledge, this is the first time to develop linear supramolecular polymers with heterometallic bicyclic metallacycles in the backbone. The conjugation length was extended after the zinc-terpyridine complexes formed, which redshifted the absorption and emission spectra. Then, a supramolecular polymer network gel was obtained by adding the cross-linker, bis-ammonium salt, to the solution of the linear supramolecular polymer. The cross-linked supramolecular polymer was found to form supramolecular gels at high concentrations in appropriate solvents, demonstrating that multi-functional smart soft materials could be accessed using the strategy developed here. Furthermore, the photophysical properties of the metallacycles and cross-linked supramolecular polymers could be effectively tuned via changing the substituents on the precursor ligands.

RESULTS AND DISCUSSION

The rhomboidal metallacycles were obtained by stirring a mixture of the 120° dipyridyl heteroditopic ligand **1a-1d** and an equimolar amount of 60° organo-diplatinum (II) acceptor **2** in DMSO-d_6 at 65 °C for 12 h. These rhomboids were pendent with benzo-21-crown-7 (B21C7) at their acute vertices and terpyridine moieties at their obtuse vertices, respectively. The detailed synthetic procedures for the ligands and metallacycles are given in the

Supporting Information (SI). These chemical structures of the ligands and the formation of discrete and highly symmetric species were confirmed by multinuclear (^{1}H and ^{31}P) NMR analyses (Figure S1–S38). Here, we use **3a** as a representative example. In the ^{1}H NMR spectrum of metallacycle **3a** (Figure 1a–1c), the protons of the pyridyl groups exhibited downfield shifts compared with those of the free ligand **1a** due to the loss of electron density upon coordination of the pyridine N atom with the platinum (II) centers. Besides, a splitting of the H_a and H_b peaks was observed (H_a from 8.68 to 9.00 and 8.90 ppm; H_b from 7.55 to 8.45 and 8.33 ppm). The assignment and correlation of the protons on the metallacycle was validated by ^{1}H-^{1}H homonuclear correlation spectroscopy (COSY) NMR experiments (Figure S29). The ^{31}P NMR spectrum of rhomboid **3a** showed a sharp singlet at 14.10 ppm with concomitant ^{195}Pt satellites ($J_{Pt\text{-}P}$ = 2678.1 Hz), in accordance with a single phosphorous environment. This peak was upfield shifted by 6.02 ppm relative to that of the platinum(II) acceptor (Figure 1d and 1e). Electrospray ionization time-of-flight mass spectrometry (ESI-TOF-MS) further demonstrated the stoichiometry of the formation of rhomboids (Figure 1f). An isotopically resolved peak corresponding to the intact and discrete [2 + 2] assembly **3a** with the loss of three trifluoromethanesulfonate (OTf^{-}) counterions was observed at m/z 1247.20 $[M - 3OTf]^{3+}$, which provided convincing evidence for the existence of the rhomboidal metallacycle as the only supramolecular species. Likewise, all other metallacycles gave the similar results as shown in the SI.

Subsequently, the linear supramolecular polymer **4a** was formed by the coordination between $Zn(OTf)_2$ and terpyridine moieties, which was investigated by UV-Vis spectroscopy. A UV-Vis titration was performed by stepwise adding a solution of $Zn(OTf)_2$ to a CH_2Cl_2/CH_3CN solution of **3a** (Figure 2a). The absorbance of the band at 392 nm corresponding to the characteristic of zinc-terpyridine complex gradually increased, and a distinct isosbestic point at 340 nm appeared, indicating the successful formation of the zinc-terpyridine complexes. As shown in Figure 2b, the absorbance at 392 nm almost remained constant after the addition of one equivalent of Zn^{2+}, indicating a 1:1 ligand-to-metal stoichiometry, which is consistent with our assumption as illustrated in Scheme 1. The binding constant K_a of Zn^{2+} and **1a** determined by UV-Vis titration is calculated to be 38000 M^{-1} (Figure S39). The linear supramolecular polymerization behavior of the monomers was then studied by various methods, including the concentration-dependent ^{1}H NMR, diffusion-ordered ^{1}H NMR spectroscopy (DOSY) and dynamic light scattering (DLS) measurements. As shown in Figure S40, by increasing the monomer concentration from 1 to 60 mM, the signals of protons H_g and H_h upfield and downfield shifted, respectively, and all the peaks of the protons became broad. As the monomer concentration increased from 5 to 60 mM, the weight-average diffusion coefficient (D) considerably decreased from 4.2×10^{-9} to 7.2×10^{-10} m^2 s^{-1}, indicating the formation of high-molecular-weight-supramolecular polymers (Figure S41a). The DLS results showed that the average hydrodynamic diameters (D_h) of the assemblies at low (2.0 mM) and high (60.0 mM) concentration were determined to be 93 and 466 nm, respectively, suggesting the generation of large aggregates in solution (Figure S41b). Moreover, a rod-like fiber was observed from the scanning electron microscopy (SEM) images, which directly supported the formation of high-molecular-weight linear supramolecular polymers (Figure S42).

Furthermore, the B21C7 units within the linear supramolecular polymer provide another platform for incorporating the third non-covalent interaction, i.e., host–guest interaction, affording a cross-linked supramolecular polymer network. Firstly, the complexation between crown ether and the secondary ammonium salt was selected as a model system to study the binding strength during supramolecular polymerization (Figure S43). The protons $H_{4'}$ and $H_{6'}$ on the bis-ammonium **5** downfield shifted, while the signals of the protons on the crown ether of **2** upfield shifted. The association constant between **2** and the mono-ammonium **7** (Figure S44) in CD_3CN/CD_2Cl_2 determined by a ^1H NMR method was 4.6 (± 1.5) × 10^2 M^{-1}, which indicated that the host-guest interaction suitable for the construction of the cross-linked supramolecular assemblies (Figure S45 and S46).

The conversion from linear to cross-linked supramolecular polymers was then accomplished by adding a bis-ammonium linker **5**. Concentration-dependent ^1H NMR measurements were performed to investigate the formation of the cross-linked supramolecular polymer as shown in Figure 3. A 1:1 mixture of **4a** and **5** was chosen as the onset. With the increasing monomer concentration, noticeable chemical shift changes for both precursors were observed. Upfield shifts were observed for the signals of H_4 and H_5 of **4a**, whereas the $H_{4'}$ and $H_{6'}$ of the bis-ammonium linker **5** shifted downfield. The peaks of all the proton signals became broader as the monomer concentrations increased, suggesting the gradual formation of the cross-linked supramolecular polymer. Furthermore, these observations also indicate that the Pt←N coordination, the terpyridine-metal coordination and the host–guest interaction don't interfere with each other in this system.

Similarly, DOSY and DLS measurements were carried out to demonstrate the formation of the cross-linked supramolecular polymer **6a** in solution. From Figure 4a, as the concentration of B21C7/ammonium salt units in the supramolecular polymer increased from 5 to 60 mM, D decreased from 2.8 × 10^{-10} to 6.2 × 10^{-11} m^2 s^{-1}. From Figure 4b, as the concentration of B21C7/ammonium salt units increased from 2 to 60 mM, D_h increased from 109 to 715 nm, which were significantly larger than those of **4a** under the same concentrations of B21C7 units (Figure S47). These results demonstrate the formation of a cross-linked supramolecular polymer. Rheological experiments on the resulting gels were also conducted to study the viscoelastic properties (Figure 4c). The storage modulus (G') is always larger than the loss modulus (G'') and both are independent of the angular frequency ω, indicative of the formation of organogels. Additionally, the SEM image as shown in Figure 4d revealed an extended and interconnected fibrous network for the xerogel prepared by a freeze-drying method, giving direct evidence for the formation of the cross-linked networks of **6a**.

The supramolecular gel exhibited gel-sol transitions triggered by thermo, K^+ and 1,4,7,10-tetraazacyclododecane (cyclen) (Figure 5). Upon heating or the addition of K^+, the gel turned into solution due to the destruction of the B21C7/secondary ammonium salt interactions. The addition of cyclen could weaken the coordination between Zn^{2+} and terpyridyl groups, accompanied with the degradation of the gel, which was evidenced by the titration UV-Vis absorption as shown in Figure S48. With the continuous addition of cyclen, the absorbance of the Zn^{2+}/terpyridyl band at 392 nm decreased. Adding 1.2 equiv. of cyclen resulted in the total disappearance of Zn^{2+}/terpyridyl absorption bands. After further

addition of equal amounts of $Zn(OTf)_2$, the absorption band at 392 reappeared. The gel could be reformed upon further cooling or the addition of 18-crown-6 (18C6) or Zn^{2+}.

The metallacycle-cored gel exhibits macroscopically self-healing properties which can be observed visually. From Figure 6, the crack on the gel with the length of 6 mm totally disappeared after 14 min. The self-healing process may be attributed to the dynamic and reversible metal coordination and host–guest interactions.

Rheological tests were also performed to study the self-healing properties (Figure 7). The gels were subjected to strain sweep tests to obtain the broken strains. As the strain exceeded 240%, G' became smaller than G'', suggesting that the gel was destroyed (Figure 7a). Then the gel was studied under large (400%) and small (0.1%) strains, respectively. As shown in Figure 7b, initially, when the strain was 400%, G'' was larger than G', indicating that the gel was broken. Subsequently, the strain was released to 0.1% and the gel was left standing for 60 s, and both G' and G'' returned to their original values. This process could be repeated for four times without any loss of the modulus. These observations indicate that the gel possesses good self-healing properties.

The optical properties of the ligands, metallacycles, linear supramolecular polymers and the cross-linked supramolecular polymers were studied by UV-Vis absorption and fluorescence spectroscopy as shown in Figure 8 and Figure S49, and the optical data are summarized in Table S1. From Figure 8, the absorption and emission maxima of the metallacycles redshift with the increase of the electron-donating ability of the substituents attached to the pyridyl ligands. Notably, **3a** with amino substituents exhibits broad emission from 400 to 750 nm. The fluorescence spectra maxima of the linear supramolecular polymers **4a** (539 nm) and **4b** (473 nm) are largely redshifted relative to those of their corresponding metallacycles **3a** (448 nm) and **3b** (430 nm), respectively, which can be attributed to the extended conjugation arising from the zinc-terpyridine coordination. The cross-linked supramolecular polymers exhibit emission wavelengths similar to those of the linear supramolecular polymers. Moreover, as shown in Figure 8c and 8d, the emission spectra of **4a** and **6a** with amino substituents present more redshifts in comparison with those of **4b** and **6b** with hydrogen substituents. These results demonstrate that the optical properties could be effectively tuned via variation of the substituents of the precursor ligands.

CONCLUSIONS

In conclusion, we have designed and constructed a new heterometallic bicyclic supramolecular polymer by means of orthogonal hierarchical self-assembly via platinum(II)-ligand coordination-driven self-assembly, zinc-terpyridine complex, and host–guest interactions. The gel obtained from high concentrations of this cross-linked supramolecular polymer exhibited dynamic properties, specifically thermo- and cation-induced sol–gel transitions. Via variation of the substituents on the precursor ligands, the optical properties of the supramolecular polymers could be effectively tuned. The combination of various metal–ligand coordination with orthogonal non-covalent interactions is a promising route to access novel supramolecular polymers with interesting and useful characteristics.

Supplementary Material

Refer to Web version on PubMed Central for supplementary material.

ACKNOWLEDGMENTS

S.Y. thanks National Natural Science Foundation of China (21971049 and 21574034) and Zhejiang Provincial Natural Science Foundation of China (ZJNSF) (LQ18B040001 and LY16B040006) for financial support. Q.Z. thanks National Natural Science Foundation of China (51703046) and China Scholarship Council for financial support. P.J.S. thanks NIH (Grant R01-CA215157) for financial support.

REFERENCES

(1). Cordier P; Tournilhac F; Soulié-Ziakovic C; Leibler L Self-Healing and Thermoreversible Rubber from Supramolecular Assembly. Nature 2008, 451, 977. [PubMed: 18288191]

(2). de Greef TFA; Meijer EW Supramolecular Polymers. Nature 2008, 453, 171. [PubMed: 18464733]

(3). Sangeetha NM; Maitra U Supramolecular Gels: Functions and Uses. Chem. Soc. Rev 2005, 34, 821. [PubMed: 16172672]

(4). Sun JY; Zhao X; Illeperuma WRK; Chaudhuri O; Oh KH; Mooney DJ; Vlassak JJ; Suo Z Highly Stretchable and Tough Hydrogels. Nature 2012, 489, 133. [PubMed: 22955625]

(5). Zhang YS; Khademhosseini A Advances in Engineering Hydrogels. Science 2017, 356, 3627.

(6). Kakuta T; Yamagishi T; Ogoshi T Stimuli-Responsive Supramolecular Assemblies Constructed from Pillar[*n*]arenes. Acc. Chem. Res 2018, 51, 1656. [PubMed: 29889488]

(7). Burnworth M; Tang L; Kumpfer JR; Duncan AJ; Beyer FL; Fiore GL; Rowan SJ; Weder C Optically Healable Supramolecular Polymers. Nature 2011, 472, 334. [PubMed: 21512571]

(8). Yang Y; Urban MW Self-Healing Polymeric Materials. Chem. Soc. Rev 2013, 42, 7446. [PubMed: 23864042]

(9). Qin B; Zhang S; Song Q; Huang Z; Xu JF; Zhang X Supramolecular Interfacial Polymerization: A Controllable Method of Fabricating Supramolecular Polymeric Materials. *Angew.* Chem. Int. Edit 2017, 56, 7639.

(10). Stuart MAC; Huck WTS; Genzer J; Müller M; Ober C; Stamm M; Sukhorukov GB; Szleifer I; Tsukruk VV; Urban M; Winnik F; Zauscher S; Luzinov I; Minko S Emerging Applications of Stimuli-Responsive Polymer Materials. Nat. Mater 2010, 9, 101. [PubMed: 20094081]

(11). Yu GC; Zhao XL; Zhou J; Mao ZW; Huang XL; Wang ZT; Hua B; Liu YJ; Zhang FW; He ZM; Jacobson O; Gao CY; Wang WL; Yu CY; Zhu XY; Huang FH; Chen XY Supramolecular Polymer-Based Nanomedicine: High Therapeutic Performance and Negligible Long-Term Immunotoxicity. J. Am. Chem. Soc 2018, 140, 8005. [PubMed: 29874067]

(12). Yan XZ; Liu ZY; Zhang QH; Lopez J; Wang H; Wu HC; Niu SM; Yan HP; Wang SH; Lei T; Li JH; Qi DP; Huang PG; Huang JP; Zhang Y; Wang YY; Li GL; Tok JBH; Chen XD; Bao ZN Quadruple H-Bonding Cross-Linked Supramolecular Polymeric Materials as Substrates for Stretchable, Antitearing, and Self-Healable Thin Film Electrodes. J. Am. Chem. Soc 2018, 140, 5280. [PubMed: 29595956]

(13). Ma C; Lu W; Yang X; He J; Le X; Wang L; Zhang J; Serpe MJ; Huang Y; Chen T Bioinspired Anisotropic Hydrogel Actuators with On–Off Switchable and Color-Tunable Fluorescence Behaviors. Adv. Funct. Mater 2018, 28, 1704568.

(14). Cui YH; Deng R; Li Z; Du XS; Jia Q; Wang XH; Wang CY; Meguellati K; Yang YW Pillar[5]Arene Pseudo[1]Rotaxane-Based Redox-Responsive Supramolecular Vesicles for Controlled Drug Release. Mater. Chem. Front 2019, 3, 1427.

(15). Yin Z; Song G; Jiao Y; Zheng P; Xu JF; Zhang X Dissipative Supramolecular Polymerization Powered by Light. CCS Chem. 2019, 1, 335.

(16). Li B; He T; Fan Y; Yuan X; Qiu H; Yin S Recent Developments in the Construction of Metallacycle/Metallacage-Cored Supramolecular Polymers via Hierarchical Self-Assembly. Chem. Commun 2019, 55, 8036.

(17). Li B; He T; Shen X; Tang D; Yin S Fluorescent Supramolecular Polymers with Aggregation Induced Emission Properties. Polym. Chem 2019, 10, 796.

(18). Yan XZ; Wang F; Zheng B; Huang FH Stimuli-Responsive Supramolecular Polymeric Materials. Chem. Soc. Rev 2012, 41, 6042. [PubMed: 22618080]

(19). Beck JB; Rowan SJ Multistimuli, Multiresponsive Metallo-Supramolecular Polymers. J. Am. Chem. Soc 2003, 125, 13922. [PubMed: 14611204]

(20). Schmatloch S; Gonzalez MF; Schubert US Metallo-Supramolecular Diethylene Glycol: Water-Soluble Reversible Polymers. Macromol. Rapid Commun 2002, 23, 957.

(21). Mei JF; Jia XY; Lai JC; Sun Y; Li CH; Wu JH; Cao Y; You XZ; Bao ZN A Highly Stretchable and Autonomous Self-Healing Polymer Based on Combination of Pt···Pt and π–π Interactions. Macromol. Rapid Commun 2016, 37, 1667. [PubMed: 27569252]

(22). Schubert US; Eschbaumer C Macromolecules Containing Bipyridine and Terpyridine Metal Complexes: Towards Metallosupramolecular Polymers. *Angew*. Chem. Int. Edit 2002, 41, 2892.

(23). Housecroft CE 4,2′:6′,4′′-Terpyridines: Diverging and Diverse Building Blocks in Coordination Polymers and Metallomacrocycles. Dalton Trans. 2014, 43, 6594. [PubMed: 24522847]

(24). Gröger G; Meyer-Zaika W; Böttcher C; Gröhn F; Ruthard C; Schmuck C Switchable Supramolecular Polymers from the Self-Assembly of a Small Monomer with Two Orthogonal Binding Interactions. J. Am. Chem. Soc 2011, 133, 8961. [PubMed: 21542617]

(25). Lee YH; He LP; Chan YT Stimuli-Responsive Supramolecular Gels Constructed by Hierarchical Self-Assembly Based on Metal-Ligand Coordination and Host-Guest Recognition. Macromol. Rapid Commun 2018, 39, 6.

(26). Li LJ; Cong Y; He LP; Wang YY; Wang J; Zhang FM; Bu WF Multiple Stimuli-Responsive Supramolecular Gels Constructed from Metal-Organic Cycles. Polym. Chem 2016, 7, 6288.

(27). Götz S; Abend M; Zechel S; Hager MD; Schubert US Platinum-Terpyridine Complexes in Polymers: A Novel Approach for the Synthesis of Self-Healing Metallopolymers. J. Appl. Polym. Sci 2019, 136, 47064.

(28). Zheng Q; Ma Z; Gong S Multi-Stimuli-Responsive Self-Healing Metallosupramolecular Polymer Nanocomposites. J. Mater. Chem A, 2016, 4, 3324.

(29). Cook TR; Stang PJ Recent Developments in the Preparation and Chemistry of Metallacycles and Metallacages via Coordination. Chem. Rev 2015, 115, 7001. [PubMed: 25813093]

(30). Fujita M; Tominaga M; Hori A; Therrien B Coordination Assemblies from a Pd(II)-Cornered Square Complex. Acc. Chem. Res 2005, 38, 369. [PubMed: 15835883]

(31). Schmitt F; Freudenreich J; Barry NPE; Juillerat-Jeanneret L; Süss-Fink G; Therrien B Organometallic Cages as Vehicles for Intracellular Release of Photosensitizers. J. Am. Chem. Soc 2012, 134, 754. [PubMed: 22185627]

(32). Clever GH; Punt P Cation–Anion Arrangement Patterns in Self-Assembled Pd_2L_4 and Pd_4L_8 Coordination Cages. Acc. Chem. Res 2017, 50, 2233. [PubMed: 28817257]

(33). Zhao C; Sun Q-F; Hart-Cooper WM; DiPasquale AG; Toste FD; Bergman RG; Raymond KN Chiral Amide Directed Assembly of a Diastereo- and Enantiopure Supramolecular Host and its Application to Enantioselective Catalysis of Neutral Substrates. J. Am. Chem. Soc 2013, 135, 18802. [PubMed: 24283463]

(34). Mendez-Arroyo J; Barroso-Flores J; Lifschitz AM; Sarjeant AA; Stern CL; Mirkin CA A Multi-State, Allosterically-Regulated Molecular Receptor With Switchable Selectivity. J. Am. Chem. Soc 2014, 136, 10340. [PubMed: 25007350]

(35). Mosquera J; Ronson TK; Nitschke JR Subcomponent Flexibility Enables Conversion between D_4-Symmetric CdII8L_8 and *T*-Symmetric CdII4L_4 Assemblies. J. Am. Chem. Soc 2016, 138, 1812. [PubMed: 26814599]

(36). Sanada K; Ube H; Shionoya M Rotational Control of a Dirhodium-Centered Supramolecular Four-Gear System by Ligand Exchange. J. Am. Chem. Soc 2016, 138, 2945. [PubMed: 26910765]

(37). Zhang Z; Zhao Z; Hou Y; Wang H; Li X; He G; Zhang M Aqueous Platinum(II)-Cage-Based Light-Harvesting System for Photocatalytic Cross-Coupling Hydrogen Evolution Reaction. Angew. Chem. Int. Edit 2019, 58, 8862.

(38). Kishi N; Akita M; Kamiya M; Hayashi S; Hsu H-F; Yoshizawa M Facile Catch and Release of Fullerenes Using a Photoresponsive Molecular Tube. J. Am. Chem. Soc 2013, 135, 12976. [PubMed: 23957216]

(39). Oliveri CG; Gianneschi NC; Nguyen ST; Mirkin CA; Stern CL; Wawrzak Z; Pink M Supramolecular Allosteric Cofacial Porphyrin Complexes. J. Am. Chem. Soc 2006, 128, 16286. [PubMed: 17165783]

(40). Xu L; Shen X; Zhou Z; He T; Zhang J; Qiu H; Saha ML; Yin S; Stang PJ Metallacycle-Cored Supramolecular Polymers: Fluorescence Tuning by Variation of Substituents. J. Am. Chem. Soc 2018, 140, 16920. [PubMed: 30465423]

(41). Zhang M; Yin S; Zhang J; Zhou Z; Saha ML; Lu C; Stang PJ Metallacycle-Cored Supramolecular Assemblies with Tunable Fluorescence Including White-Light Emission. Proc. Natl. Acad. Sci. U. S. A 2017, 114, 3044. [PubMed: 28265080]

(42). Zhang M; Saha ML; Wang M; Zhou Z; Song B; Lu C; Yan X; Li X; Huang F; Yin S; Stang PJ Multicomponent Platinum(II) Cages with Tunable Emission and Amino Acid Sensing. J. Am. Chem. Soc 2017, 139, 5067. [PubMed: 28332834]

(43). Li ZY; Zhang Y; Zhang C-W; Chen L-J; Wang C; Tan H; Yu Y; Li X; Yang HB Cross-Linked Supramolecular Polymer Gels Constructed from Discrete Multi-pillar[5]arene Metallacycles and Their Multiple Stimuli-Responsive Behavior. J. Am. Chem. Soc 2014, 136, 8577. [PubMed: 24571308]

(44). Shi B; Liu Y; Zhu H; Vanderlinden RT; Shangguan L; Ni R; Acharyya K; Tang J-H; Zhou Z; Li X; Huang F; Stang PJ Spontaneous Formation of a Cross-Linked Supramolecular Polymer Both in the Solid State and in Solution, Driven by Platinum(II) Metallacycle-Based Host–Guest Interactions. J. Am. Chem. Soc 2019, 141, 6494. [PubMed: 30966741]

(45). Chen LJ; Yang HB Construction of Stimuli-Responsive Functional Materials via Hierarchical Self-Assembly Involving Coordination Interactions. Acc. Chem. Res 2018, 51, 2699. [PubMed: 30285407]

(46). Zheng W; Yang G; Shao NN; Chen LJ; Ou B; Jiang ST; Chen GS; Yang HB CO_2 Stimuli-Responsive, Injectable Block Copolymer Hydrogels Cross-Linked by Discrete Organoplatinum(II) Metallacycles via Stepwise Post-Assembly Polymerization. J. Am. Chem. Soc 2017, 139, 13811. [PubMed: 28885839]

(47). Hu X-Y; Xiao T; Lin C; Huang F; Wang L Dynamic Supramolecular Complexes Constructed by Orthogonal Self-Assembly. Acc. Chem. Res 2014, 47, 2041. [PubMed: 24873508]

(48). Yan X; Li S; Cook TR; Ji X; Yao Y; Pollock JB; Shi Y; Yu G; Li J; Huang F; Stang PJ Hierarchical Self-Assembly: Well-Defined Supramolecular Nanostructures and Metallohydrogels via Amphiphilic Discrete Organoplatinum(II) Metallacycles. J. Am. Chem. Soc 2013, 135, 14036. [PubMed: 23927740]

(49). Yan X; Cook TR; Pollock JB; Wei P; Zhang Y; Yu Y; Huang F; Stang PJ Responsive Supramolecular Polymer Metallogel Constructed by Orthogonal Coordination-Driven Self-Assembly and Host/Guest Interactions. J. Am. Chem. Soc 2014, 136, 4460. [PubMed: 24621148]

(50). Lu C; Zhang M; Tang D; Yan X; Zhang Z; Zhou Z; Song B; Wang H; Li X; Yin S; Sepehrpour H; Stang PJ Fluorescent Metallacage-Core Supramolecular Polymer Gel Formed by Orthogonal Metal Coordination and Host-Guest Interactions. J. Am. Chem. Soc 2018, 140, 7674. [PubMed: 29856215]

(51). Zhou Z; Yan X; Cook TR; Saha ML; Stang PJ Engineering Functionalization in a Supramolecular Polymer: Hierarchical Self-Organization of Triply Orthogonal Non-covalent Interactions on a Supramolecular Coordination Complex Platform. J. Am. Chem. Soc 2016, 138, 806. [PubMed: 26761393]

(52). Sepehrpour H; Saha ML; Stang PJ Fe–Pt Twisted Heterometallic Bicyclic Supramolecules via Multicomponent Self-Assembly. J. Am. Chem. Soc 2017, 139, 2553. [PubMed: 28151656]

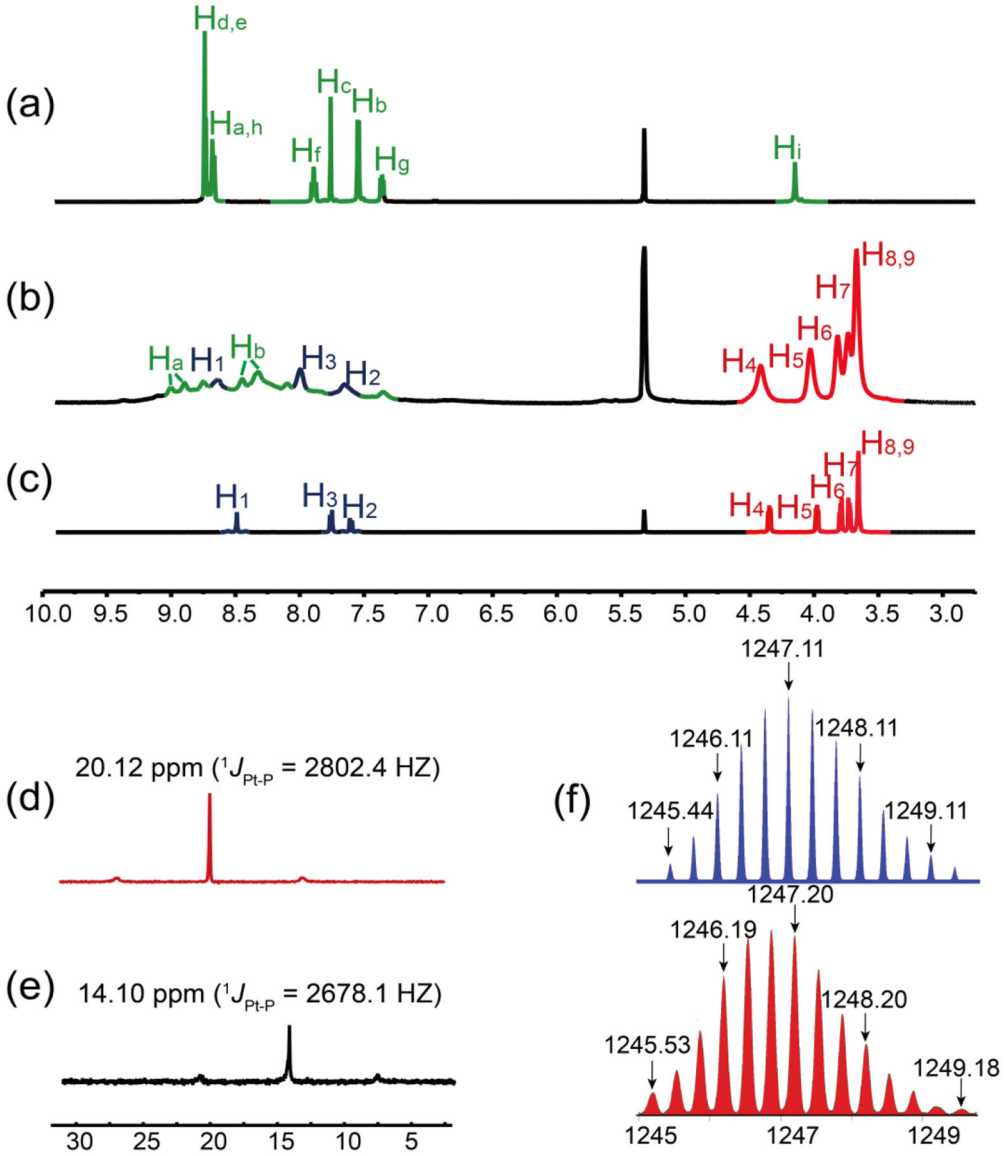

Figure 1.

Partial (a-c) ^{1}H and (d, e) ^{31}P NMR spectra [CD_3CN/CD_2Cl_2 (1:1, *v*/*v*), 295 K] of (a) **1a**, (b, e) **3a**, (c, d) acceptor **2**. (f) Experimental (red) and calculated (blue) ESI-TOF-MS spectra of rhomboidal metallacycle **3a** $[M - 3OTf]^{3+}$.

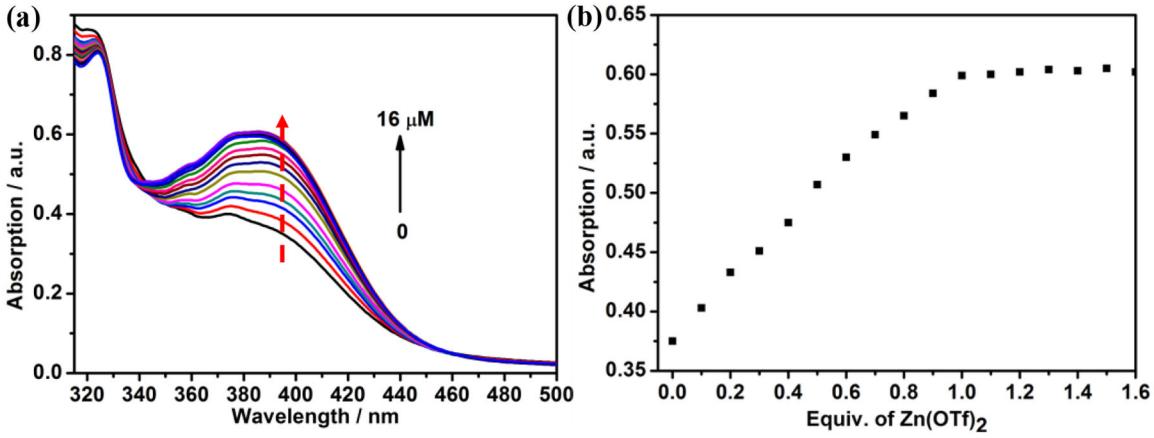

Figure 2.

(a) Change in the absorption spectra upon stepwise addition of $Zn(OTf)_2$ to **3a** in CH_2Cl_2/CH_3CN (1/1, *v/v*); (b) Plot of the absorbance at 392 nm versus the amount of $Zn(OTf)_2$.

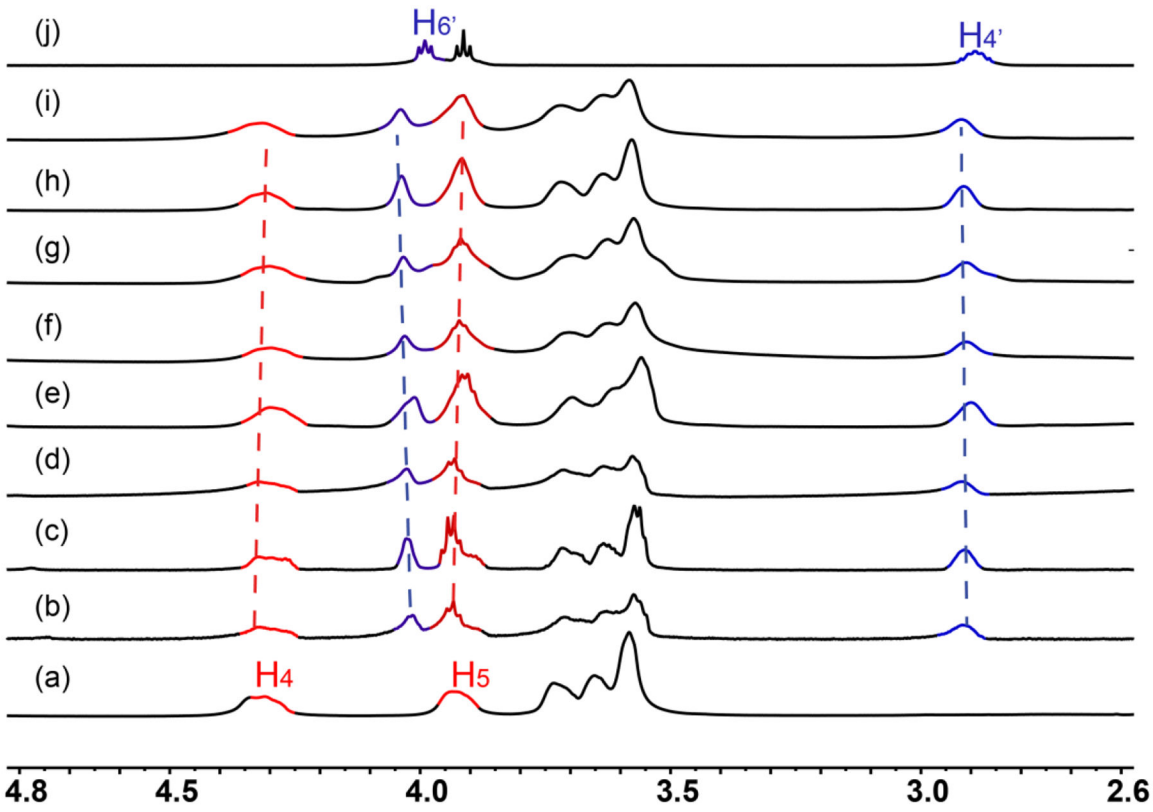

Figure 3.

Partial ^{1}H NMR spectra (CD_3CN/CD_2Cl_2, 1/1, *v/v*, 295 K, 500 MHz) of (a) **4a**, (j) **5** and (b-i) **6a** (or 1:1 mixture of **4a** and **5**) at the concentration of B21C7 unit of (b) 1 mM (c) 5 mM (d) 10 mM (e) 20 mM (f) 30 mM (g) 40 mM (h) 50 mM (i) 60 mM.

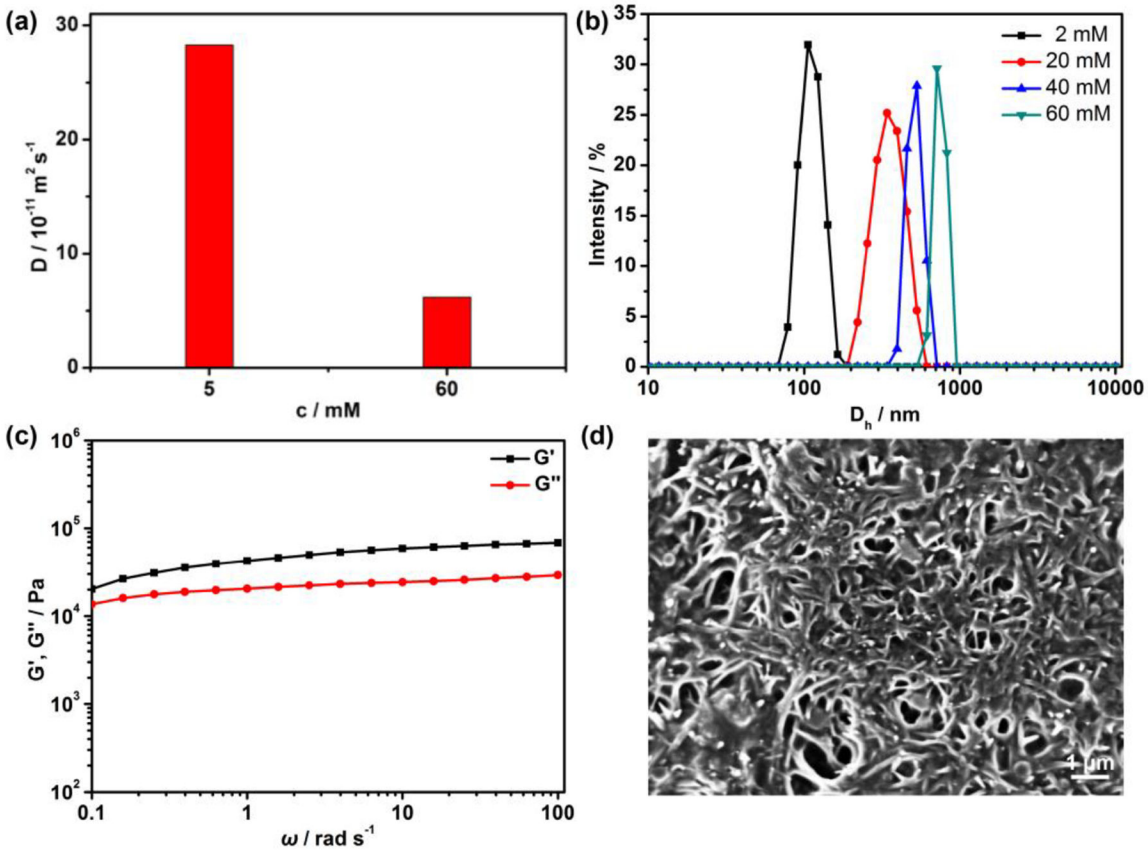

Figure 4.

(a) Concentration dependence of diffusion coefficient D (CD_3CN/CD_2Cl_2 = 1/1, *v/v*, 295 K, 400 MHz) of **6a**; (b) Size distributions of **6a** at different concentrations of B21C7 units in the mixture of CH_3CN/CH_2Cl_2 (1/1, *v/v*); (c) G' and G'' versus ω for the gel with the concentration of B21C7 unit of 240 mM in CH_3CN/CH_2Cl_2 (1/1, *v/v*); (d) SEM image of **6a** with the concentration of B21C7 unit of 10 mM in CH_3CN/CH_2Cl_2 (1/1, *v/v*). The scale bar is 1 μm.

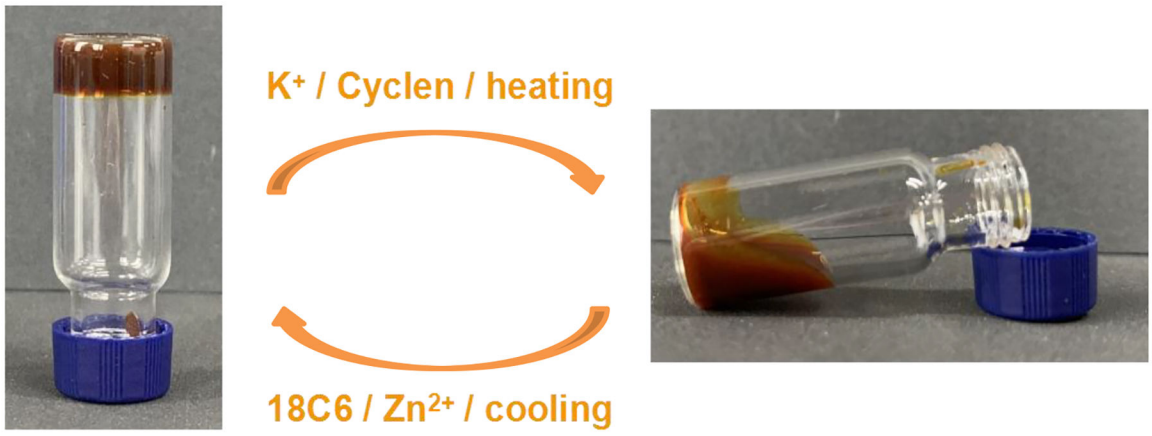

Figure 5.

Optical photographs of the reversible gel–sol transition of the supramolecular network with the concentration of B21C7 unit of 240 mM in CH_3CN/CH_2Cl_2 (1/1, *v/v*).

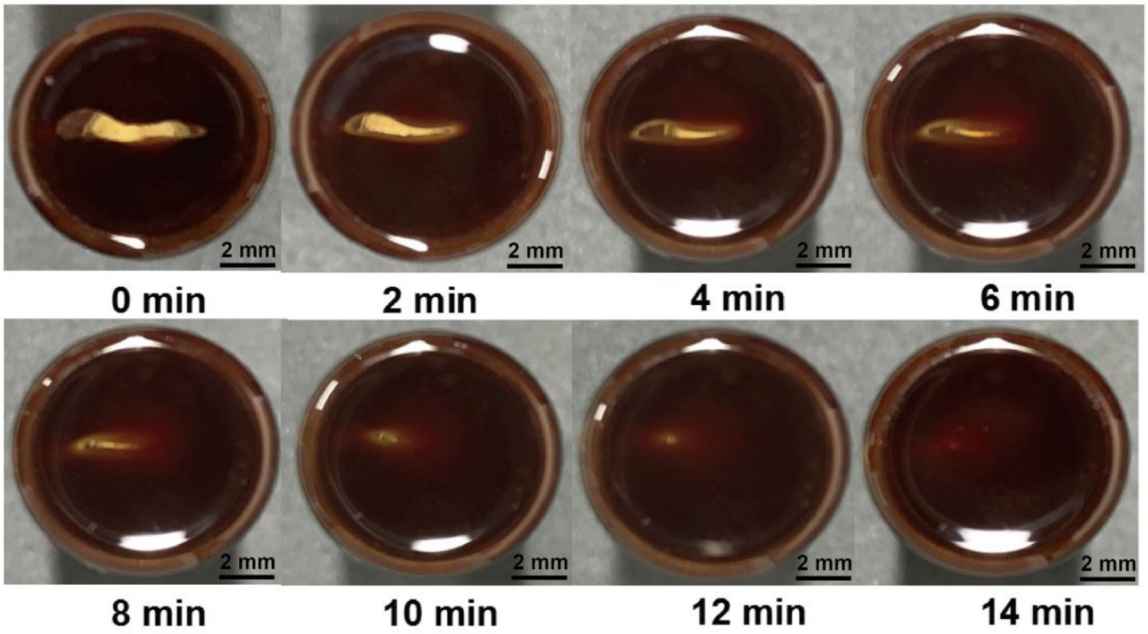

Figure 6.

Photographs of the self-healing process of the supramolecular gel with the concentration of B21C7 unit of 240 mM in CH_3CN/CH_2Cl_2 (1/1, *v/v*). The gel was cut and left standing for 2 min, 4 min, 6 min, 8 min, 10 min, 12 min and 14 min, respectively.

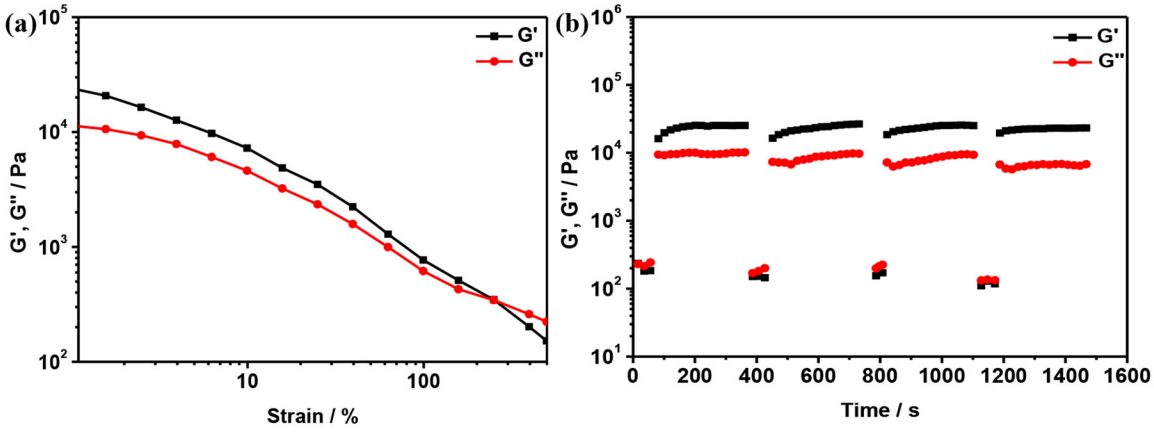

Figure 7.

(a) *G*' and *G*'' versus strain sweep. (b) Gel in continuous step-strain measurements. The gel with the concentration of B21C7 unit of 240 mM in CH_3CN/CH_2Cl_2 (1/1, *v/v*) was subjected to 400% strain for 60 s, then back to 0.1% strain and retained for 60 s, in the linear regime for 300 s, and four cycles were done.

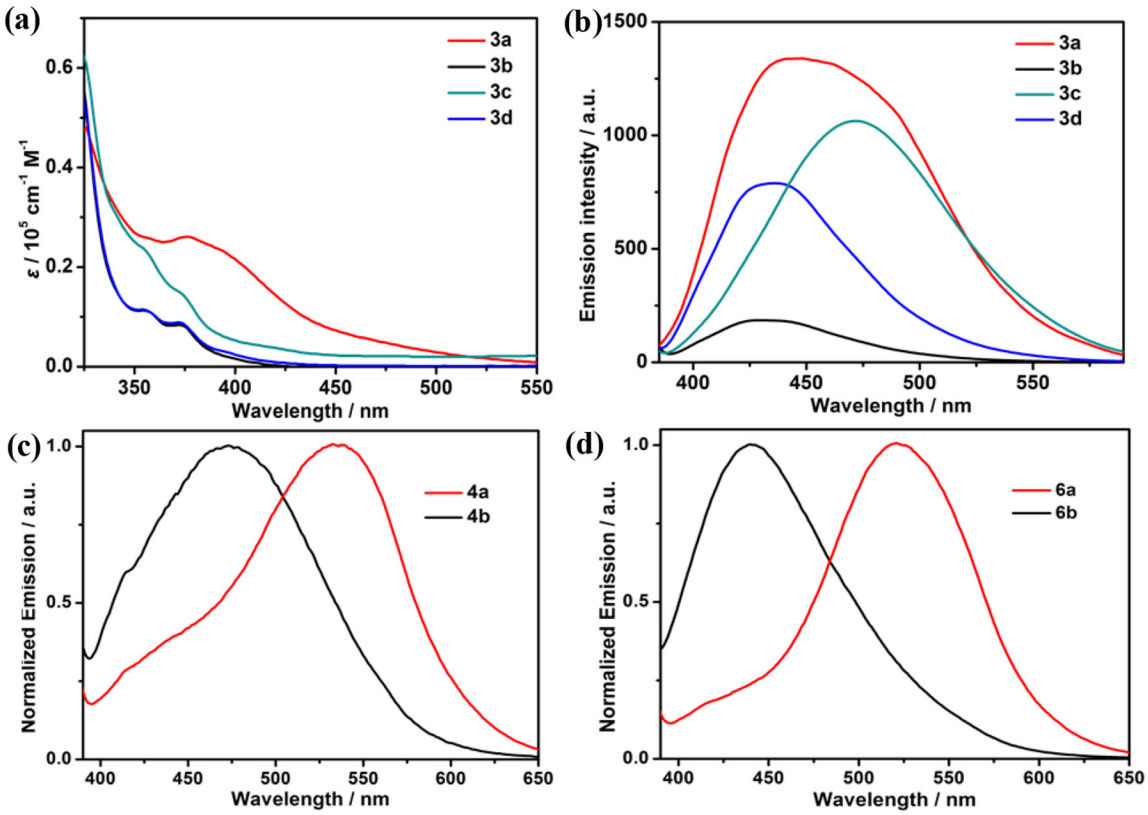

Figure 8.

(a) Absorption and (b) emission spectra of metallacycles **3a-3d**. Normalized emission spectra of (c) **4a** and **4b**, and (d) **6a** and **6b**.

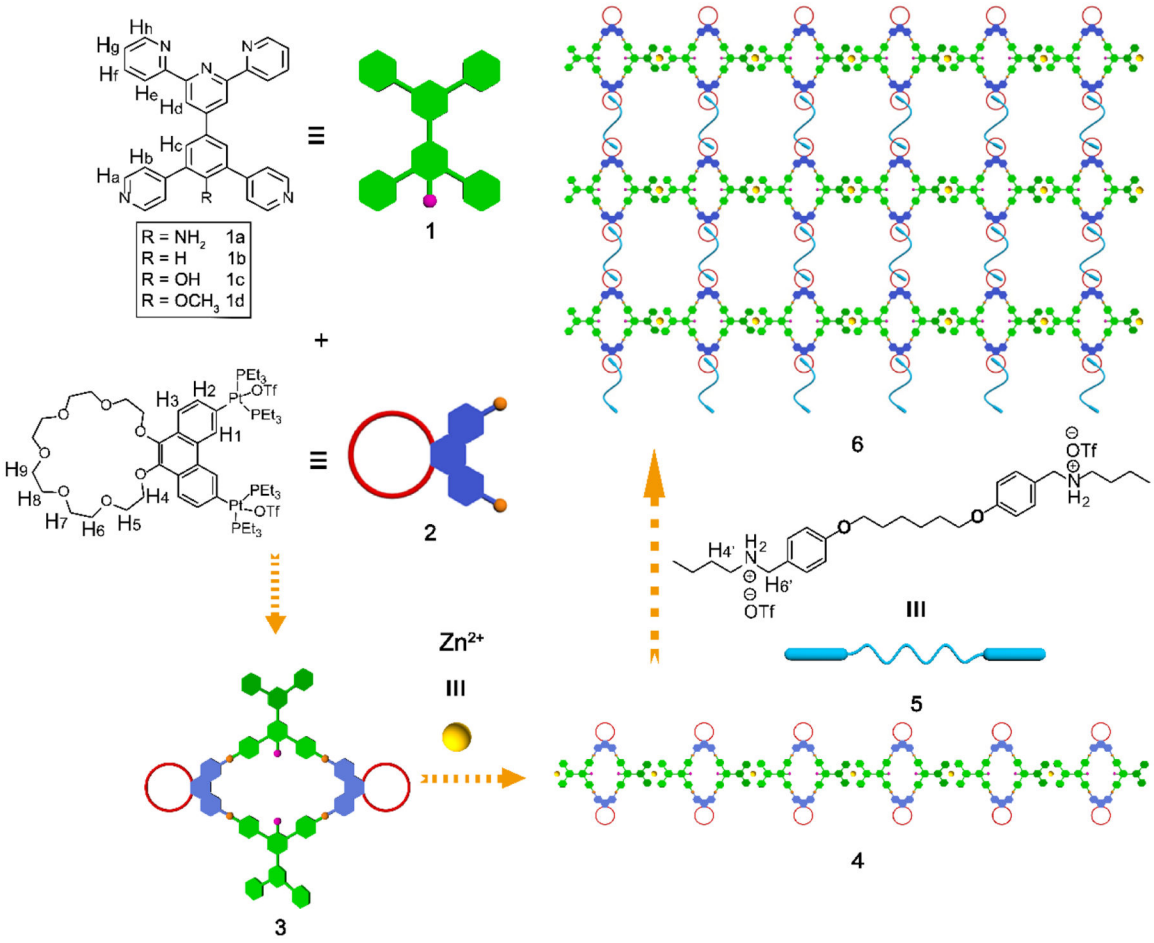

Scheme 1.

Cartoon representation of the formation of rhomboidal metallacycles, a linear supramolecular polymer and a cross-linked 3D supramolecular polymeric network from metallacycles, Zn^{2+} and bis-ammonium salts.